processes

MDPI

Article

Depolymerization and Hydrogenation of Organosolv Eucalyptus Lignin by Using Nickel Raney Catalyst

Massimo Morgana, Egidio Viola, Francesco Zimbardi *, Nadia Cerone, Assunta Romanelli and Vito Valerio

ENEA—Department of Energy Technologies and Renewable Energy Sources, Research Center of Trisaia, S.S.106 Jonica, km 419 +500, 75026 Rotondella, MT, Italy; massimo.morgana@enea.it (M.M.); egidio.viola@enea.it (E.V.); nadia.cerone@enea.it (N.C.); assunta.romanelli@enea.it (A.R.); vito.valerio@enea.it (V.V.)

* Correspondence: francesco.zimbardi@enea.it

Abstract: The use of lignocellulosic biomass to obtain biofuels and chemicals produces a large amount of lignin as a byproduct. Lignin valorization into chemicals needs efficient conversion processes to be developed. In this work, hydrocracking of organosolv lignin was performed by using nickel Raney catalyst. Organosolv lignin was obtained from the pretreatment of eucalyptus wood at 170 °C for 1 h by using 1/100/100 (*w*/*v*/*v*) ratio of biomass/oxalic acid solution (0.4% *w*/*w*)/1-butanol. The resulting organic phase of lignin in 1-butanol was used in hydrogenation tests. The conversion of lignin was carried out with a batch reactor equipped with a 0.3 L vessel with adjustable internal stirrer and heat control. The reactor was pressurized at 5 bar with hydrogen at room temperature, and then the temperature was raised to 250 °C and kept for 30 min. Operative conditions were optimized to achieve high conversion in monomers and to minimize the loss of solvent. At the best performance conditions, about 10 wt % of the lignin was solubilized into monomeric phenols. The need to find a trade-off between lignin conversion and solvent side reaction was highlighted.

Keywords: lignin; catalytic conversion; hydrogen

Citation: Morgana, M.; Viola, E.; Zimbardi, F.; Cerone, N.; Romanelli, A.; Valerio, V. Depolymerization and Hydrogenation of Organosolv Eucalyptus Lignin by Using Nickel Raney Catalyst. *Processes* **2021**, *9*, 1093. https://doi.org/10.3390/pr9071093

Academic Editor: Carmen Boeriu

Received: 27 April 2021
Accepted: 17 June 2021
Published: 23 June 2021

1. Introduction

The need to drastically reduce the exploitation of nonrenewable resources in favor of renewable ones is widely recognized. The acceleration of climate change due to the greenhouse gases released into the atmosphere requires the rules on which our economy is based to be rewritten. Lignocellulosic biomass is one of the most studied renewable sources for sustainably replacing petroleum in obtaining fuels and chemicals.

Lignocellulosic biomass is composed of three intertwined polymers: cellulose (40–50 wt %), hemicellulose (25–30 wt %), and lignin (15–20 wt %); the exact composition is strictly dependent on the origin and type of biomass [1].

Cellulose and hemicellulose can be isolated and transformed into a variety of chemicals or fuels through several methodologies [1–5].

Lignin is a complex three-dimensional amorphous polymer composed of three main phenylpropane units (coniferyl, sinapyl, and p-coumaryl alcohols) connected by β–O–4′, β–5′, β–β′, β–1′, 5–5′, and 5–O–4′ linkages in addition to several different minor phenolic compounds, and its structure and composition is dependent on the plant. The complexity and degree of polymerization make it impossible to find two lignins with the same sequence of phenyl units; for this reason, it is more appropriate to refer to "lignins" [6,7]. Due to the recalcitrance of lignin to be degraded, it is typically a waste that is combusted to produce heat and power. On the other hand, lignin is the most abundant renewable source composed of aromatic units in nature and it is worth finding a sustainable way to use it as feedstock to produce intermediates for the chemical industry and high-value liquid fuels.

For this reason, in recent years, there has been an increased interest in lignin, evidenced by the exponential increase in scientific publications related to its valorization [8].

The depolymerization of lignin is the first step to transform it into valuable products for industry. The main transformation strategies developed to date can be grouped into biochemistry, thermochemistry, and chemistry. The biochemical route focuses on the biological conversion of lignin and its derivatives to high-value products using bacteria, fungi, and enzymes [9–20]. Thermochemistry applied to lignin can be divided into oxidative, reductive, pyrolytic, hydrolytic, and gasification processes [9,19,21–26]. Hydrolysis, hydroprocessing, and oxidation are used in the chemistry-based route. A number of catalysts can be used in all these processes to increase yields and selectivity [9,19,21–23,25,27–33].

Metal catalysts and supported metal catalysts were employed in the presence of hydrogen to convert lignin into monomers in hydrogenolysis and hydrogenation processes. The most used catalytic systems are Pd/C, Ni/C, Pt/C, Pt/Al_2O_3, Cu-based porous oxides, supported NiW, NiMo, Ru-based materials, Ni-Ru, Ni-Rh, Ni-Pd, Ni-Au, WP, Ru_xNi1_{-x}/SBA-15, Al-SBA-15, MoO_x/CNT, and $S_2O_8{}^{2-}$-KNO_3/TiO_2 [9,21,25,31–35].

The Ni/Al alloy was utilized as starting material to produce a catalyst in novel hydrogenolysis: this was obtained exposing Ni, the active phase, by etching Al atoms in an alkaline aqueous solution [36]. Lignin depolymerization and product hydrogenation were tested using Ni/SiO_2 catalyst under mild condition [37]. Formic acid, as an in situ hydrogen source, and Ru/C as a catalyst in supercritical ethanol were tested to depolymerize lignin into a high-quality bio-oil; the combination of Ru/C and formic acid also resulted in a significant reduction of the oxygen content in the products [38]. New catalysts such as $S_2O_8{}^{2-}$-KNO_3/TiO_2 were synthesized and studied for the hydrocracking of lignin to improve the efficiency of the process and selectively target the formation of products [39]. The competition between hydrogenolysis and hydrodeoxygenation with the repolymerization was investigated in metallic catalysts of $CrCl_3$ and Pd/C [40]. The hydroconversion of a wheat straw soda lignin with a $NiMoS/Al_2O_3$ catalyst was studied to resolve the reaction network [41].

A. McVeigh et al. investigated the depolymerization of lignin over a Pt/alumina catalyst, and they reported a clear solvent effect [42]. The measured high yield of monomers was attributed to the inhibition of repolymerization by methanol. The depolymerization reaction was also studied over Rh/alumina and Ir/alumina catalysts, indicating that there was considerable potential in optimizing the solvent system for lignin depolymerization.

Nickel Raney has been widely used as a catalyst for the hydrothermal conversion of lignin. Struven and Meier tested several nickel Raney catalysts in aqueous media with organosolv lignin at high temperature and pressure under H_2 atmosphere to produce selectively highly reactive phenol and its para- or ortho-alkylated derivatives in high yields [43].

Organosolv lignin, a coproduct of the organosolv process, constitutes a process stream that can be upgraded through catalytic hydrogenation for the production of monomers and oligomers with higher added value [40,43–53].

The aim of this work was to use this catalyst to improve the economic sustainability of the lignin conversion into monomeric phenols. Thermal hydrocracking of organosolv lignin, originating directly from the pretreatment stream, was performed in alcoholic media under hydrogen atmosphere and mild conditions of temperature and pressure. A donor hydrogen solvent other than water was tested with this catalyst to explore its potential.

2. Materials and Methods

2.1. Lignin Extraction and Reaction System

The organosolv lignin was obtained from ground eucalyptus treated with 1-butanol and oxalic acid at temperature of 170 °C for 60 min. The extraction was carried out in 300 mL Parr reactor loaded with 5 g of eucalyptus dry matter, 50 mL of 1-butanol, and 50 mL of oxalic acid solution 0.167 M, under stirring condition at 400 rpm. The obtained slurry was filtered and the cellulosic fraction was washed with water. The two liquid phases were separated by a separator funnel and the butanol phase (lighter) was used for the

hydrocracking tests. The dry matter in the organic fraction was determined by keeping the sample at 60 °C overnight; it was 2.1% w/w. All used reagents were of pure grade.

Hydrocracking tests were performed using 300 mL Parr reactor (from Büchi, model Limbo-li, Essen, Germany) equipped with a 0.3 L vessel. About 30 g of organosolv lignin solution was added with 10 g 1-butanol containing a nickel Raney catalyst as a slurry 10% w/w of solid in alcoholic solution (purchased from Sigma, St. Louis, MO, USA). After swiping the freeboard volume with H_2 to remove air, the reactor was pressurized at 5.5 bar with H_2 at room temperature. In the experimental runs, two parameters were changed: temperature, in the range 260–300 °C, and time, in the range 30–90 min. At the end of the runs, the reactor was cooled down, and solution and gases were recovered and analyzed. The full procedure is schematized in Figure 1, while Figure 2 shows the Parr reactor and the experimental setup.

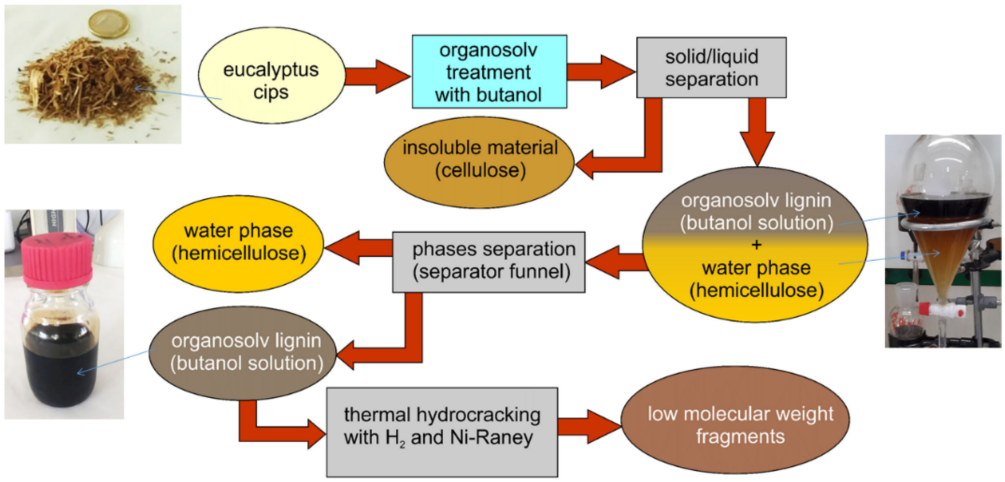

Figure 1. Process scheme.

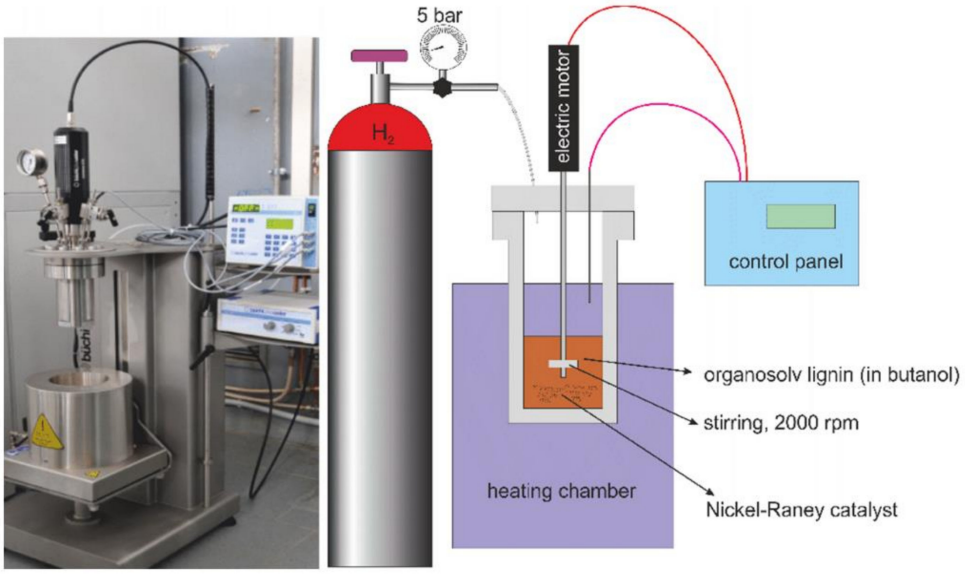

Figure 2. Parr reactor picture and scheme of the experimental setup.

2.2. Analytical Methods

Lignin solution was analyzed by HPLC (Agilent 1100 series) with the GPC columns SUPELCO TSKgel-G4000HHR, TSKgel-G3000HHR, and TSKgel-G2500HHR to determine molecular weights and GC-MS (Agilent 6890N equipped with MSD5975B) with Agilent 5MS 30 m to analyze the molecules produced after hydrocracking. Guaiacol was used as internal standard for quantitative analysis. Produced gases were collected in bags at the end of the experimental run and analyzed by Micro GC Agilent 3000 series with PLOTQ and Molsieve columns.

2.3. Experimental Design

The hydrocracking tests were set up following an experimental design (Design expert 10) where 2 parameters were varied:

- Temperature, °C, in the range 260–300;
- Time, minutes, in the range 30–90.

The study options were as follows:

- Study Type: Response Surface;
- Design Type: Central Composite;
- Subtype: Randomized;
- Design Model: Quadratic.

By using these options, the software algorithm produced 10 runs with 2 center points (Figure 3).

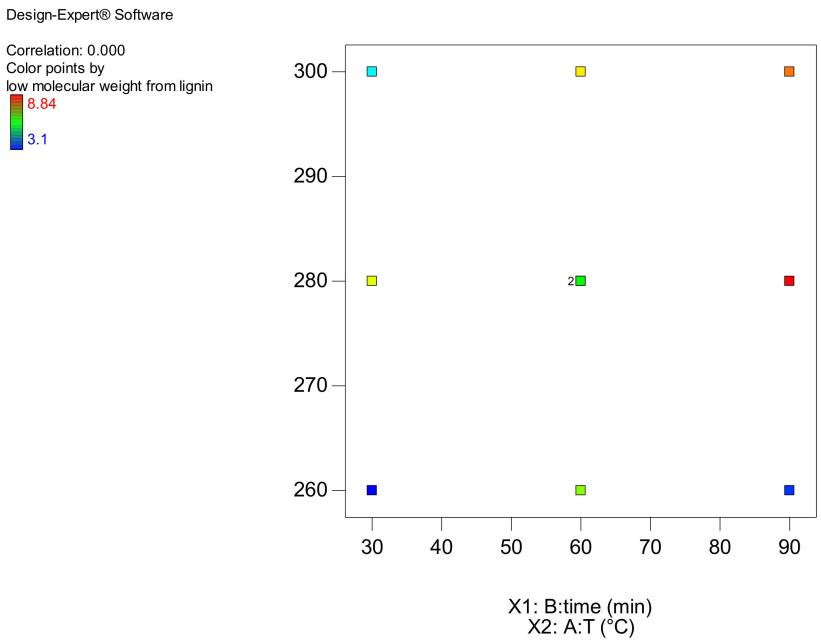

Figure 3. Matrix of the experimental runs.

3. Results and Discussion

The extracted lignin, dissolved in butanol, constituted 27.5 wt % of the starting dry eucalyptus, with a purity of up to 70% estimated by thermogravimetric analysis (TGA).

Thermal hydrocracking of organosolv lignin, catalyzed by nickel Raney, converts lignin and part of the solvent into low-weight molecules and gases. The 1-butanol, used as solvent, has a critical pressure of 44 ± 1 bar and a critical temperature of 289 ± 2 °C [54]; all tests at 260 and 280 °C were performed below critical temperature and above critical pressure, whereas tests at 300 °C were carried out under supercritical conditions. Among the monomers derived from the lignin and determined by CG, the main components that were detected as responses to different testing conditions are reported in

Table 1. These constituted the input data for the analysis of the experimental design and the following process optimization. The design was analyzed for each response; surfaces that correlated the predicted response to the variables were shown, allowing the determination of trends and the best conditions to use in order to obtain the desired values.

3.1. Response 1: Diphenylmethane 4-ethyl

In Figure 4a the correlation between the actual values (Table 1) and those predicted by the analysis is shown. In this case, the correlation factor is R^2 = 0.7120; therefore, any conclusion about the trend is qualitative. In Figure 5, the surface graph shows the variation of the response with the examined variables. The analysis of the diphenylmethane shows that the maximum production is predicted at 280 °C and at a lower time (30–35 min). At these conditions, 3% of lignin is expected to be converted into this component.

Table 1. Monomeric phenols produced from lignin at different hydrocracking conditions. Responses 1–4 report the yield of the monomers [1]. Response 5 reports yield as wt % of the loaded solvent mass.

	Factor 1	**Factor 2**	**Response 1**	**Response 2**	**Response 3**	**Response 4**	**Response 5**
Run	T	time	Diphenyl-methane 4-ethyl	2,4-Dimethyl-3-(methoxy-carbonyl)-5-ethylfuran	1,2,3-Trimethoxy benzene	Total of main monomeric compounds [2]	Molecules derived from solvent [3]
	°C	min	wt %	wt %	wt %	wt %	wt %
1	260	30	1.62	0.61	0.87	3.1	0.0432
2	260	60	2.43	1.37	1.29	6.74	0.124
3	280	90	2.08	2.48	1.67	8.84	0.281
4	260	90	1.8	0.56	0.691	3.39	0.125
5	300	90	2.49	1.49	1.56	8.18	0.478
6	300	60	2.36	1.27	1.61	7.5	0.307
7	280	30	3.05	1.15	1.42	7.27	0.175
8	280	60	2.4	1.11	1.3	6.51	0.25
9	300	30	1.56	0.853	1.03	4.51	0.116
10	280	60	1.99	1.34	1.44	6	0.182

[1] Calculated as (weight of monomer/weight of loaded lignin) × 100. The weight of the monomer is determined by its concentration × the volume of liquid phase. [2] Contains also guaiacol, syringol, p-ethylguaiacol, 2-metossi, 4-propyl phenol. [3] Butyl butanoate, 2-ethyl-2-hexenal, 2-ethyl-1-hexanol, 7-methyl-4-octanone.

3.2. Response 2: 2,4-Dimethyl-3-(methoxycarbonyl)-5-ethylfuran

In Figure 4b, the correlation between the actual values (Table 1) and those predicted by the analysis is shown. Similarly to above, R^2 = 0.7604; therefore, any conclusions about the trend are qualitative. In Figure 6, the surface graph shows the variation of the response with the examined variables. The analysis shows that max production is predicted at 284 °C and at the highest time (90 min). At these conditions, about 2.2% of this component is predicted to be produced.

3.3. Response 3: 1,2,3-Trimethoxy Benzene

In Figure 4c, the correlation between the actual values (Table 1) and those predicted by the analysis is shown. In Figure 7, the surface graph shows the variation of the response with the examined variables. The analysis shows that the max production is predicted at 296 °C and at the highest time (90 min). At these conditions, about 1.7% is expected to be converted into this component.

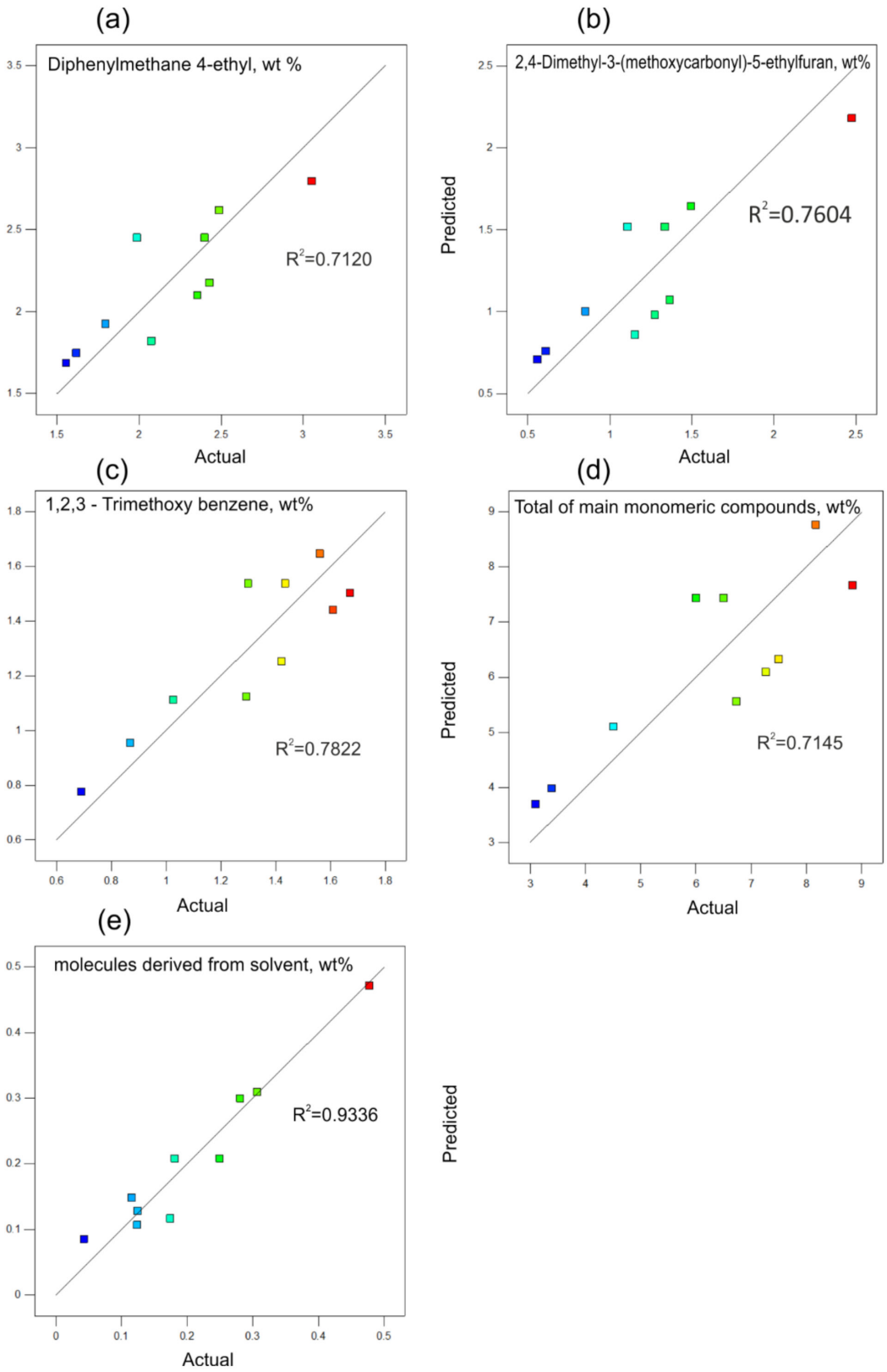

Figure 4. Predicted molecule production vs experimental values. (**a**) Response 1; (**b**) Response 2; (**c**) Response 3; (**d**) Response 4; (**e**) Response 5 (see Table 1).

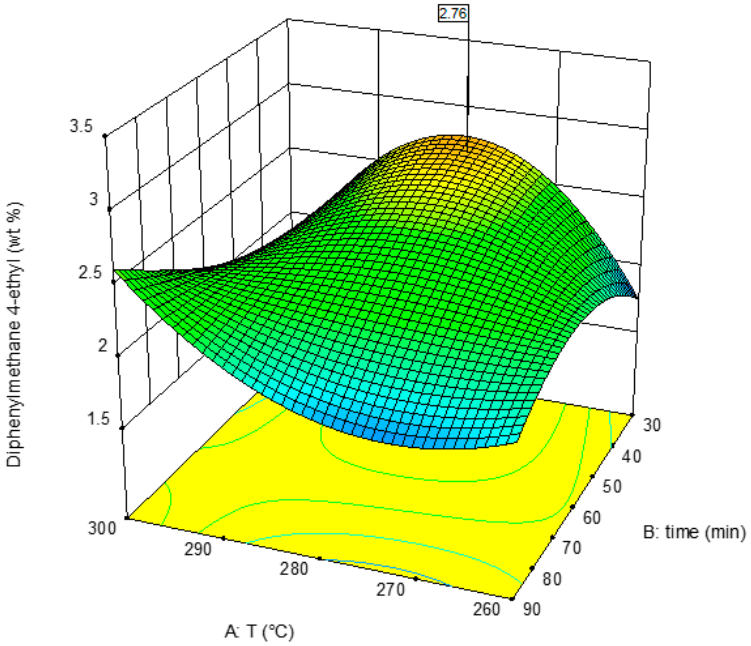

Figure 5. Prediction of the diphenylmethane production at different conditions of temperature and residence time.

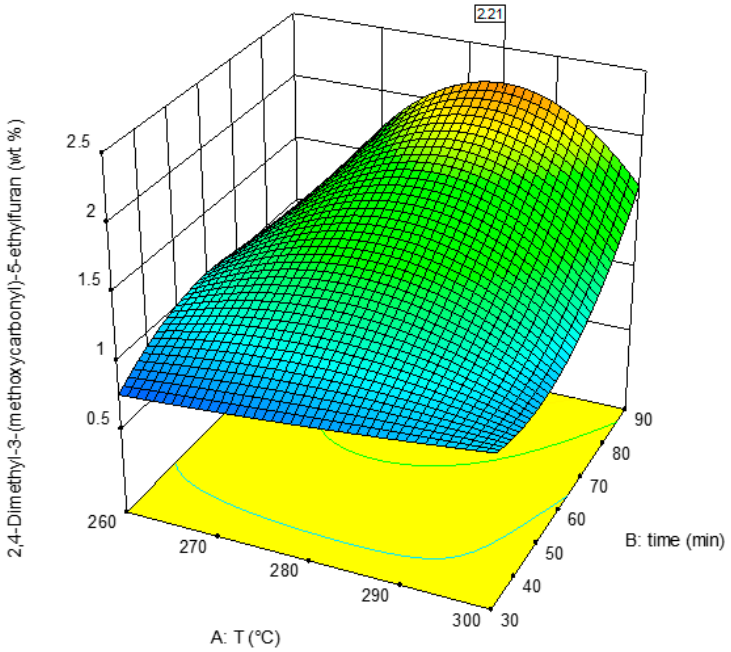

Figure 6. Prediction of the 2,4-dimethyl-3-(methoxycarbonyl)-5-ethylfuran production at different conditions of temperature and residence time.

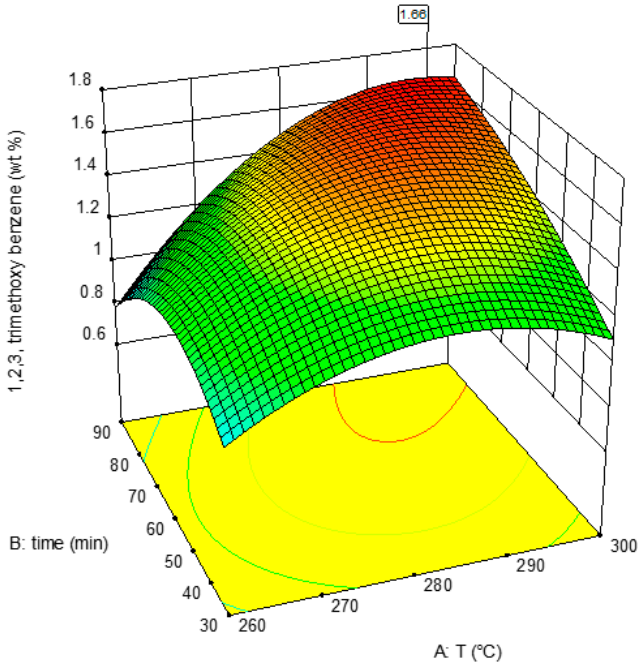

Figure 7. Prediction of the 1,2,3-trimethoxy benzene production at different conditions of temperature and residence time.

3.4. Response 4: Total of Main Monomeric Compounds

In this analysis, we considered the sum of the identified monomers by GC-MS database (over 80% matching), including the first three responses plus guaiacol, syringol, p-ethylguaiacol, 2-methoxy, and 4-propyl phenol (the last four compounds were produced with an average contribution of 0.05%, 0.1%, 0.3%, and 0.3%, respectively). In Figure 4d, the correlation between the actual values (Table 1) and those predicted by the analysis is shown. In this case, the correlation factor R^2 is 0.7145; therefore, any conclusions about the trend are qualitative. In Figure 8, the surface graph shows the variation of the response with the examined variables. The analysis shows that the max production is predicted at 296 °C and at the highest time (90 min). At these conditions, the production of the main monomers is predicted to be about 9% (as wt % with respect to the solubilized lignin).

3.5. Response 5: Molecules Derived from Solvent

In this response, we considered the sum of the identified monomers by GC-MS database derived from solvent: butyl butanoate, 2-ethyl-2-hexenal, 2-ethyl-1-hexanol, and 7-methyl-4-octanone. The amount, reported in Table 1, is the percent mass yield of loaded solvent. In Figure 4e, the correlation between the actual values (Table 1) and those predicted by the analysis is shown. In this case, the correspondence factor R^2 is 0.9336, and therefore the considerations about the trend are quantitatively significant. In Figure 9, the surface graph shows the variation of the response with the examined variables. The analysis shows that the max production is predicted at 300 °C and at the highest time (90 min). At these conditions, about 0.5 wt % of the solvent is converted in these molecules.

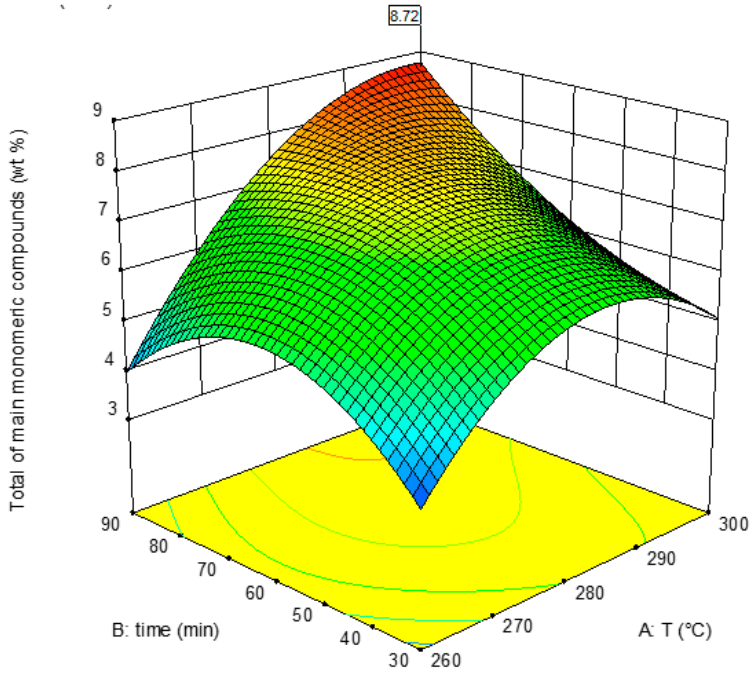

Figure 8. Prediction of the production of the monomeric compounds at different conditions of temperature and residence time.

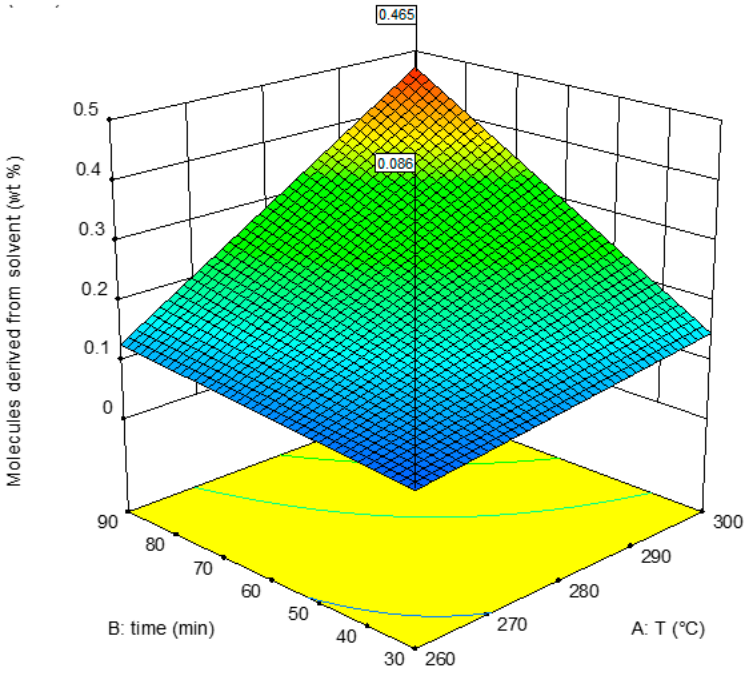

Figure 9. Prediction of the production of the molecules derived from the solvent at different conditions of temperature and residence time.

3.6. Optimization

The optimization process has taken into account that our goal was to maximize the production of low-molecular-weight molecules from the lignin and, at the same time, to save energy by operating at low temperature and shorter time. We also expected solvent consumption to be reduced to a minimum. For this reason, the criteria shown in Table 2 were ranked as input according to their importance in reaching the goal.

Table 2. Criteria used for reaction parameter optimization.

Constraints				
Name	**Goal**	**Lower Limit**	**Upper Limit**	**Importance**
A:T	minimize	260	300	1
B:time	minimize	30	90	1
Diphenylmethane 4-ethyl	maximize	1.56	3.05	5
2,4-Dimethyl-3-(methoxycarbonyl)-5-ethylfuran	maximize	0.56	2.48	5
1,2,3-Trimethoxy benzene	maximize	0.691	1.67	5
Total of main monomeric compounds	maximize	3.1	8.84	5
Molecules derived from solvent	minimize	0.0432	0.478	3

Following the constraints reported in Table 2, the software (Design Expert 10) elaborated the solution shown in Table 3, where the best parameters to adopt in the examined hydrocracking process are located near the center point of the test matrix (279 °C and 60 min). Figure 10 shows the position of the desired solution in the contour plot for each response. Under optimized conditions, we can observe that, compared to a 15% yield reduction (in the total number of monomers produced at the highest conditions), the temperature and time are reduced (respectively by 21 °C and 30 min). Moreover, the production of monomers derived from the solvent decreased by 57% wt.

Table 3. Selected solution for the best operational condition.

T	time	Resp1	Resp2	Resp3	Resp4	Resp5	Desirability
278.6	60.5	2.444	7.412	1.529	1.527	0.202	0.645

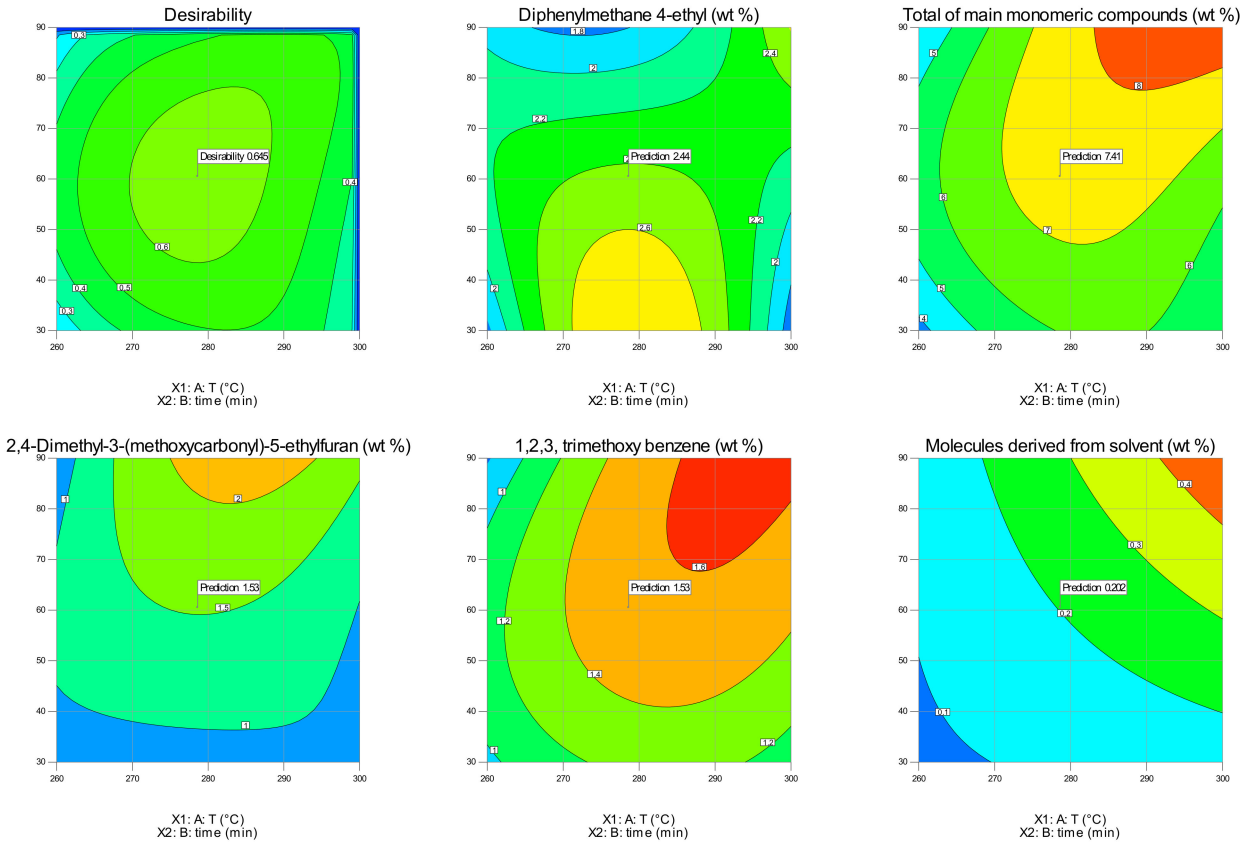

Figure 10. Position of the desired solution in the contour plot for each response.

3.7. Gas Analyses

The following gases were detected in the gas phase after the hydrogenation: carbon monoxide, carbon dioxide, methane, ethane, and propane. Generally, the most abundant was propane, followed by carbon dioxide and methane, with a common trend for all tests (Figure 11). The increase in temperature and reaction time increased the amount of produced gases, reported in Figure 11 as wt % of the total starting organic solution. Consumption of solvent was large at severe conditions as shown by the large amount converted into gases. Table 4 reports the calculated mass balance of the process at the different conditions and shows that the consumption of solvent transformed into gas became relevant under the most severe conditions; for instance, 53% was converted at 300 °C and 90 min of reaction.

Table 4. Mass balance at the end of the experimental runs based on the total mass recovered.

Run	T, °C	t, min	Solution Recovery [1], wt %	Produced Gas [2], wt %	Mass Balance [3]
1	260	30	90.5	3.4	0.939
2	260	60	83.6	10.6	0.942
3	260	90	84.0	9.2	0.932
4	280	30	84.2	11.3	0.95.5
5	280	60	60.6	24.1	0.847
6	280	60	64.2	16.5	0.807
7	280	90	47.5	43.2	0.907
8	300	30	51.6	22.7	0.743
9	300	60	44.4	41.6	0.856
10	300	90	36.4	52.6	0.890

The wt % of final liquid and solid with respect to the starting solution. [2] The wt % of recovered gas with respect to the starting solution (sum of CO, CO_2, CH_4, C_2H_6, C_3H_8). [3] $\sum mass_{out} / \sum mass_{in}$.

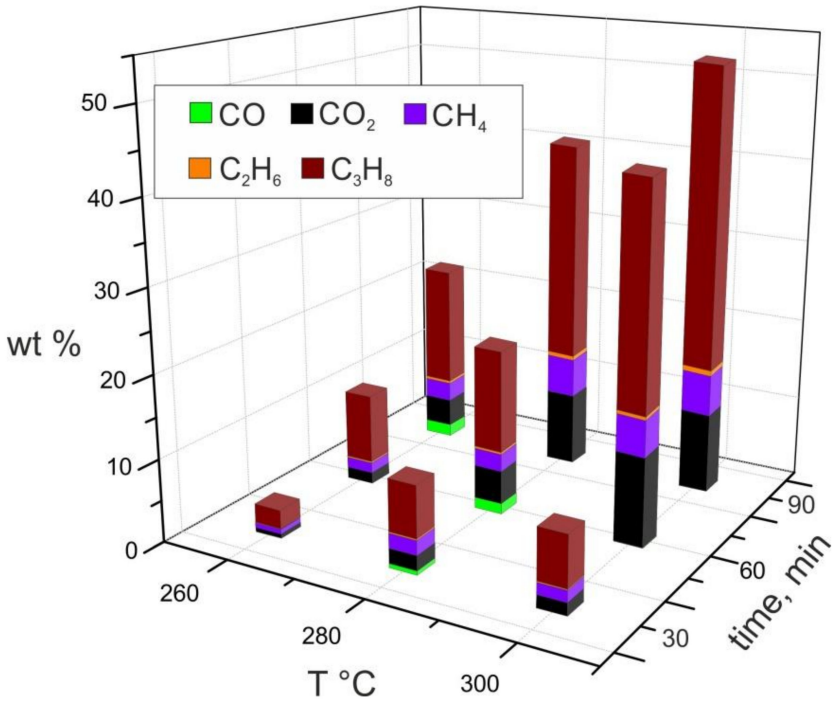

Figure 11. Amount of produced gases at different temperatures and residence times.

3.8. HPLC-GPC Analyses

The organosolv lignin and organic solution obtained after hydrocracking were analyzed by HPLC to determine the obtained fragments and their molecular weights. The chromatogram of organosolv lignin showed molecular weights under 5500 dalton (Figure 12). The peak in the chromatogram at very low molecular weight was due to impurity in butanol, as deduced from the chromatogram obtained with a light scattering detector. After the reaction of hydrocracking, almost all fragments had molecular weights below the 1100 dalton, with the main peaks of the distribution below 350 dalton, corresponding to trimers, dimers, and monomers. It was inferred that more severe conditions increased the production of molecules having low molecular weight, as expected. Chromatograms at different wavelengths (220.4, 273.4, 254.4, and 320.4 nm) were obtained with similar results.

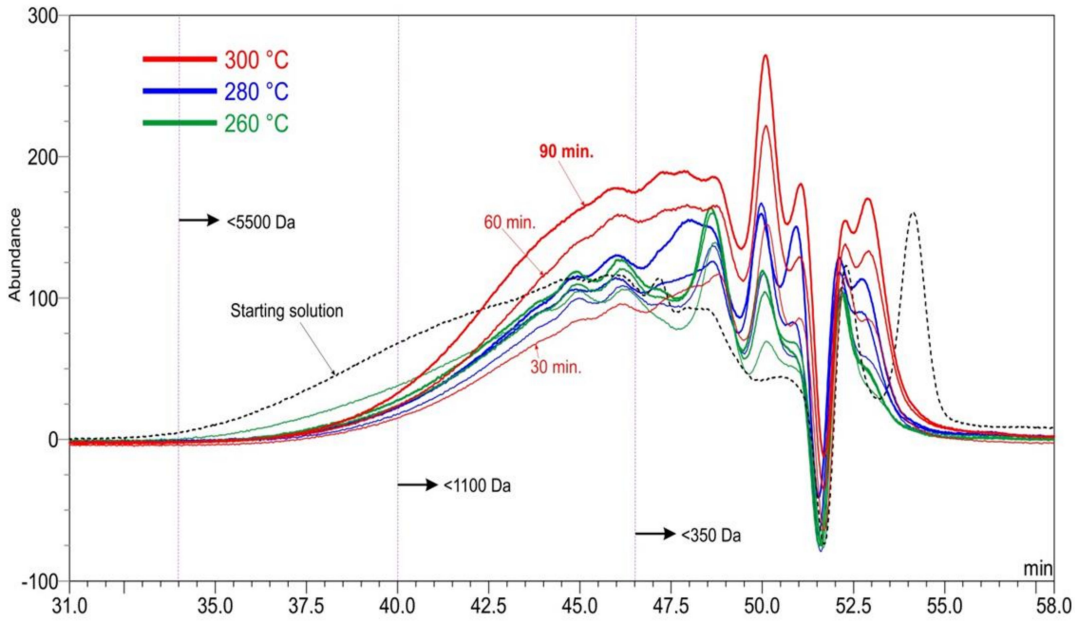

Figure 12. Chromatograms at the wavelength of 214.4 nm by HPLC with GPC column before (dashed line) and after hydrocracking at different temperatures and residence times (colored lines).

Longer residence times of reaction led to the difference being amplified, especially at high temperature, with an increased production of molecules with low molecular weight. At low temperature, there was a negligible difference between chromatograms. There was a regular correlation between the increase in reaction severity, in particular with the temperatures, and the production of molecules having low molecular weight.

The results obtained are compared with other works reported in the literature in Table 5. A larger quantity of monomers is obtained with noncommercial catalysts and higher temperatures, reaching 80% of yield using bifunctional catalysts [45] or much more severe conditions such as 100 bar of H_2, 400 °C, and 240 min [47]. A detailed economic analysis should be performed to select the most convenient catalyst and solvent, including for example the recycling of products, catalyst cost and life, and byproducts. This is evidently out of the scope of this paper, which is focused on highlighting the role of the solvent used in the butanol-based organosolv pretreatment and one of the cheapest catalysts on the market, the Ni Raney.

Table 5. Literature review of organosolv lignin hydroprocessing.

H_2 (bar)	T, (°C)	Time, (min)	Catalyst	Solvent	Products	Yield [1] (%)	Ref.
5	279	60	Raney Nickel	butanol	monomers	7.4	This work
40	280	300	Pd/C, Pd/C+$CrCl_3$	methanol	monomers	~45	40
75	360	180	Raney Nickel	water	monomers	25	43
180	400	120	NiMo	oils	phenols	12.8	44
10	130	120	$Ni_{85}Ru_{15}$	water	monomers	80	45
40	140	1200	Cu-PMO	methanol	catechols	63.7	46
100	400	240	Ru/TiO_2	–	Lignin oil	78	47
20	320	360	Ni/zeolites	hexadecane	hydrocarbons	70	48
50	400	49	Pd/C	ethanol	monomers	13	50
20	240	240	Pd/C	ethanol	monomers	~17	53

[1] (Weight of products/weights of lignin)·100. Best reported results.

3.9. Kinetic Analysis

The production data of aromatic monomers and nongaseous degradation products of the solvent were processed to determine the activation energy of the reactions. The kinetic expression of a reaction catalyzed by solids can be very complex, especially considering the mass transfer between the phases, which in this case are (1) hydrogen gas in equilibrium with (2) the liquid solution and (3) the solid catalyst dispersed in the liquid phase. Furthermore, the diffusion in the pores of the reactants and products should also be considered according to the chemical theory [55]. An elementary kinetic model was assumed, based on first-order reactions to empirically describe the set of reactions that occur as in the scheme shown in Figure 13. From a mechanistic point of view, this assumption corresponds to identifying only one limiting step in the overall kinetic process, which we could identify in the breaking of the intermolecular bond β-O-4.

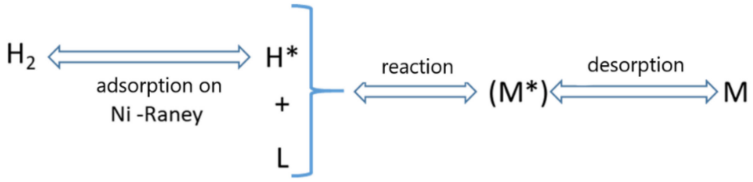

Figure 13. Reaction scheme related to the catalytic hydrogenation of lignin. L = lignin, M = monomers, * = activated state.

The tests were designed and performed to minimize diffusion effects between liquid bulk and catalyst by operating at high stirring speed and breaking the diffusion film. Furthermore, the nickel Raney had negligible porosity. Under these conditions, a kinetic regime can reasonably be assumed.

As the conversion rate of the lignin, *L*, generically produces a monomer *M*, the reaction can be indicated as reported in Equation (1).

$$r = -\frac{dL}{dt} = \frac{dM}{dt} \quad (1)$$

The instantaneous rate of global reaction of *L*, a reagent that gradually decreases, with hydrogen H_2 can be assumed proportional to the concentration of the reactants and to the surface of the catalyst, *S*, as shown in Equation (2).

$$r = -k\,S[L][H_2] \quad (2)$$

The concentration of hydrogen in the liquid, $[H_2]$, can be approximated as constant because it is in equilibrium with the gaseous phase loaded with excess pressure of hydrogen gas. The surface of the catalyst, *S*, can also be considered constant:

$$\frac{d[L]}{dt} = -K[L] \quad (3)$$

Then, with the constant k of the Arrhenius type being calculated as in Equation (4), the logarithmic relationship is obtained (Equation (5)).

$$k = k_o\, e^{-\frac{Ea}{RT}} \quad (4)$$

$$ln\frac{d[L]}{[L]} = \mathrm{lnK} + \ln Ao - \frac{Ea}{RT} \quad (5)$$

By plotting the logarithm of the specific reaction speed $d[L]/L$ as a function of the inverse of the absolute temperature at which these reaction rates are measured, a straight line is obtained from whose angular coefficient the value of Ea can be obtained (Figure 14, Table 6).

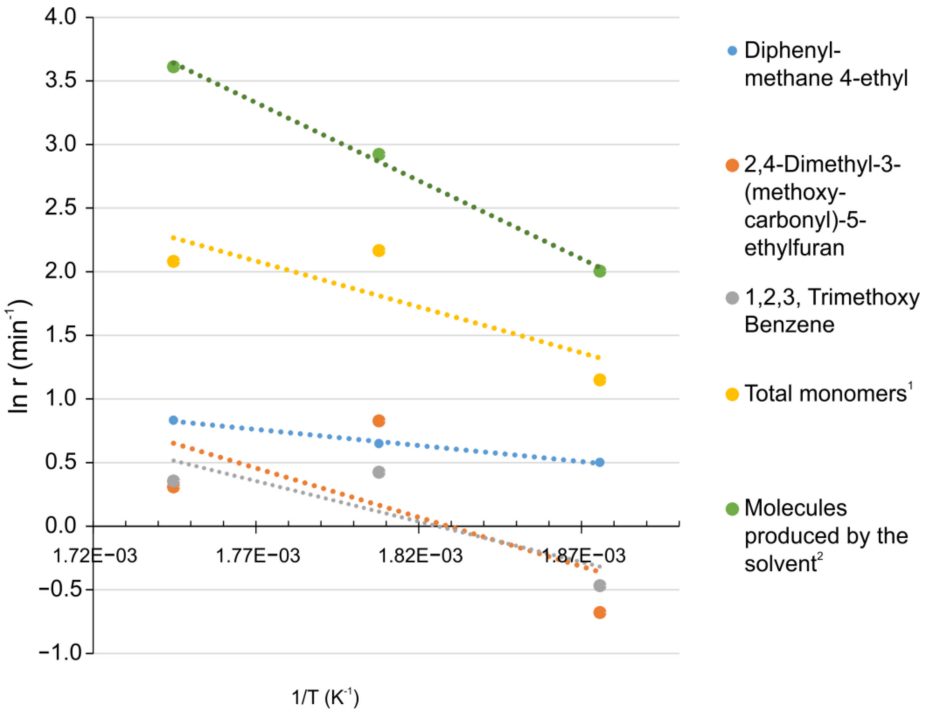

Figure 14. Arrhenius diagram of the catalytic conversion of lignin corresponding to a 90 min test. [1] Contains also guaiacol, syringol, p-ethylguaiacol, 2-metossi, 4-propyl phenol. [2] Butyl butanoate, 2-ethyl-2-hexenal, 2-ethyl-1-hexanol, 7-methyl-4-octanone.

Table 6. Activation energies for the conversion of lignin and solvent to monomers to nongaseous organic compounds.

	Diphenyl-methane 4-ethyl	2,4-Dimethyl-3-(methoxy-carbonyl)-5-ethylfuran	1,2,3-Trimethoxy Benzene	Total Monomers [1]	Molecules Produced by the Solvent [2]
Ea, kJ/mol	21.0	64.3	53.0	60.0	102.1

[1] Contains also guaiacol, syringol, p-ethylguaiacol, 2-metossi, 4-propyl phenol. [2] Butyl butanoate, 2-ethyl-2-hexenal, 2-ethyl-1-hexanol, 7-methyl-4-octanone.

The data in Table 1 were elaborated to obtain the average conversion rates for three single monomer species and for the total of monomers. In order to minimize the effect of thermal transients and errors on analytical measurements (higher at lower concentrations), the data corresponding to the maximum reaction time, 90 min, were considered. The elaborations are shown in Figure 14, where the ordinates show the average specific rate

of formation in the time range 0–90 min and the x-axis shows the inverse of the absolute temperatures at which the tests were performed.

The activation energy values obtained by linear regression are reported in Table 6 and vary from 21 kJ mol^{-1} (diphenyl-methane 4-ethyl) to 64.3 kJ mol^{-1} (2,4-dimethyl-3-(methoxy-carbonyl)-5-ethylfuran), while for the total monomers, an average value of 60.0 kJ mol^{-1} was obtained. Compared to the energy of the β-O-4 bond (150 kJ mol^{-1}), the activation energy is considerably lower due to the action of the catalyst and in accordance with recent research concerning the hydrogenation and hydrodeoxygenation of lignin monomers with carbon-supported Ni catalysts [56].

In the Arrhenius diagram in Figure 14, the straight line relating to the decomposition of butanol to nongaseous compounds (butyl butanoate, 2-ethyl-2-hexenal, 2-ethyl-1-hexanol, 7-methyl-4-octanone) had a better correlation coefficient, probably due to the minor experimental error in the determination of molecules with higher concentration. The activation energy was 102.1 kJ mol^{-1}, in accordance with what was reported for the decomposition of butanol at 270 °C in thermal desorption studies in TGA [57] and with the kinetics of alkene dehydration detected in the pyrolysis of n-butanol in continuous reactors at 700 K [58]. The decomposition of butanol into more elementary molecules (H_2, C_nH_m, CO_x) was, however, the predominant reaction, especially at high temperatures, as described in the literature, in the case of reforming in the presence of nickel Raney [59].

4. Conclusions

Thermal treatment of organosolv lignin with hydrogen and nickel Raney catalyst in subcritical and critical condition of 1-butanol solvent depolymerizes the lignin, and oxygenated trimers, dimers, and monomers can be obtained. The conversion in monomers reached 9 wt %, though this value is limited to the identified molecules ((diphenyl-methane 4-ethyl, 2,4-dimethyl-3-(methoxycarbonyl)-5-ethylfuran, and trimethoxy benzene), and higher yields could be obtained. The hydrogenation and cracking reactions also involve the solvent, and its use increases with the temperature and time. When also taking into account the desired minimization of solvent consumption between 20 and 35 wt %, the optimized conditions were found to be 279 °C and 60 min, with a monomeric yield of 7.4 wt %. The role of the reaction medium strongly suggests the need for further research to find a suitable trade-off between solvent type and monomer yield making the whole process sustainable.

Compared to other catalytic systems, such as those based on bifunctional catalysts [45], the Ni Raney catalyst appears low-performing. However, a full process analysis should be performed to establish which would be the more convenient option to be used, taking into consideration factors such as the recycling options or the capital cost of operating at more severe conditions [47].

Author Contributions: Conceptualization, F.Z., M.M., and E.V.; methodology, V.V., and A.R.; software, E.V., and M.M.; validation, F.Z., E.V., and M.M.; formal analysis, N.C.; investigation, M.M., andnd A.R.; resources, F.Z.; data curation, M.M., F.Z., and E.V.; writing—original draft preparation, F.Z., M.M., and E.V.; visualization, E.V.; project administration F.Z., and N.C.; funding acquisition, F.Z. All authors have read and agreed to the published version of the manuscript.

Funding: This research was funded by EC, grant number 731101.

Institutional Review Board Statement: N.A.

Informed Consent Statement: N.A.

Data Availability Statement: N.A.

Acknowledgments: The authors thank Maria A. Cerone for the language revision.

Conflicts of Interest: The authors declare no conflict of interest.

References

1. Kumar, A.A.; Rapoport, A.; Kunze, G.; Kumar, S.; Singh, D.; Singh, B. Multifarious pretreatment strategies for the lignocellulosic substrates for the generation of renewable and sustainable biofuels: A review. *Renew. Energy* **2020**, *160*, 1228–1252.
2. Qaseem, M.F.; Shaheen, H.; Wu, A.-M. Cell wall hemicellulose for sustainable industrial utilization. *Renew. Sustain. Energy Rev.* **2021**, *144*, 110996. [CrossRef]
3. Banwell, M.G.; Pollard, B.; Liu, X.; Connal, L.A. Exploiting Nature's Most Abundant Polymers: Developing New Pathways for the Conversion of Cellulose, Hemicellulose, Lignin and Chitin into Platform Molecules (and Beyond). *Chem. Asian J.* **2021**, *16*, 604–620. [CrossRef] [PubMed]
4. Robak, K.; Balcerek, M. Current state-of-the-art in ethanol production from lignocellulosic feedstocks. *Microbiol. Res.* **2020**, *240*, 126534. [CrossRef] [PubMed]
5. Meneses, D.B.; de Oca-Vásquez, G.M.; Vega-Baudrit, J.R.; Rojas-Álvarez, M.; Corrales-Castillo, J.; Murillo-Araya, L.C. Pretreatment Methods of Lignocellulosic Wastes into Value-Added Products: Recent Advances and Possibilities. *Biomass Convers. Biorefinery* **2020**, *1*, 1–18.
6. Banoub, J.; Delmas, G., Jr.; Joly, N.; Mackenzie, G.; Cachet, N.; Benjelloun-Mlayah, B.; Delmas, M. A critique on the structural analysis of lignins and application of novel tandem mass spectrometric strategies to determine lignin sequencing. *J. Mass Spectrom.* **2015**, *50*, 5–48. [CrossRef]
7. Achyuthan, K.E.; Achyuthan, A.M.; Adams, P.D.; Harper, S.M.J.C.; Simmons, B.A.; Singh, A.K. Supramolecular Self-Assembled Chaos: Polyphenolic Lignin's Barrier to Cost-Effective Lignocellulosic Biofuels. *Molecules* **2010**, *15*, 8641–8688. [CrossRef]
8. Abejón, R.; Pérez-Acebo, H.; Clavijo, L. Alternatives for Chemical and Biochemical Lignin Valorization: Hot Topics from a Bibliometric Analysis of the Research Published During the 2000–2016 Period. *Process* **2018**, *6*, 98. [CrossRef]
9. Poveda-Giraldo, J.A.; Solarte-Toro, J.C.; Alzate, C.A.C. The potential use of lignin as a platform product in biorefineries: A review. *Renew. Sustain. Energy Rev.* **2021**, *138*, 110688. [CrossRef]
10. Dikshit, P.K.; Jun, H.-B.; Kim, B.S. Biological conversion of lignin and its derivatives to fuels and chemicals. *Korean J. Chem. Eng.* **2020**, *37*, 387–401. [CrossRef]
11. Singh, S.K. Biological treatment of plant biomass and factors affecting bioactivity. *J. Clean. Prod.* **2021**, *279*, 123546. [CrossRef]
12. Dashtban, M.; Schraft, H.; Syed, T.A.; Qin, W. Fungal biodegradation and enzymatic modification of lignin. *Int. J. Biochem. Mol. Biol.* **2010**, *1*, 36–50. [PubMed]
13. Bugg, T.D.; Ahmad, M.; Hardiman, E.M.; Singh, R. The emerging role for bacteria in lignin degradation and bio-product formation. *Curr. Opin. Biotechnol.* **2011**, *22*, 394–400. [CrossRef] [PubMed]
14. Galebach, P.; Mcclelland, D.J.; Eagan, N.M.; Wittrig, A.M.; Buchanan, J.S.; Dumesic, J.A.; Gasser, C.A.; Hommes, G.; Schäffer, A.; Corvini, P.F.X. Multi-catalysis reactions: New prospects and challenges of biotechnology to valorize lignin. *Appl. Microbiol. Biot* **2012**, *95*, 1115–1134.
15. Brown, M.E.; Chang, M.C. Exploring bacterial lignin degradation. *Curr. Opin. Chem. Biol.* **2014**, *19*, 1–7. [CrossRef]
16. Roth, S.; Spiess, A.C. Laccases for biorefinery applications: A critical review on challenges and perspectives. *Bioprocess. Biosyst. Eng.* **2015**, *38*, 2285–2313. [CrossRef]
17. Husarcíková, J.; Voß, H.; Domínguez de María, P.; Schallmey, A. Microbial β-etherases and glutathione lyases for lignin valorisation in biorefineries: Current state and future perspectives. *Appl. Microbiol. Biotechnol.* **2018**, *102*, 5391–5401. [CrossRef]
18. Xu, R.; Zhang, K.; Liu, P.; Han, H.; Zhao, S.; Kakade, A.; Khan, A.; Du, D.; Li, X. Lignin Depolymerization and Utilization by Bacteria. *Bioresour. Technol.* **2018**, *269*, 557–566. [CrossRef]
19. Chio, C.; Sain, M.; Qin, W. Lignin utilization: A review of lignin depolymerization from various aspects. *Renew. Sustain. Energ. Rev.* **2019**, *107*, 232–249. [CrossRef]
20. Weng, C.; Peng, X.; Han, Y. Depolymerization and conversion of lignin to value-added bioproducts by microbial and enzymatic catalysis. *Biotechnol. Biofuels* **2021**, *14*, 84. [CrossRef]
21. Pandey, M.P.K.; Kim, C.S. Lignin depolymerization and conversion: A review of thermochemical methods. *Chem. Eng. Technol.* **2011**, *34*, 29–41. [CrossRef]
22. Azadi, P.; Inderwildi, O.R.; Farnood, R.; King, D.A. Liquid fuels, hydrogen and chemicals from lignin: A critical review. *Renew. Sustain. Energ. Rev.* **2013**, *21*, 506–523. [CrossRef]
23. Davis, K.; Rover, M.; Brown, R.; Bai, X.; Wen, Z.; Jarboe, L. Recovery and Utilization of Lignin Monomers as Part of the Biorefinery Approach. *Energies* **2016**, *9*, 808. [CrossRef]
24. Xu, L.J.; Zhang, Y.; Fu, Y. Advances in upgrading lignin pyrolysis vapors by ex situ catalytic fast pyrolysis. *Energy Technol.* **2017**, *5*, 30–51. [CrossRef]
25. Li, C.; Zhao, X.; Wang, A.; Huber, G.H.; Zhang, T. Catalytic transformation of lignin for the production of chemicals and fuels. *Chem. Rev.* **2015**, *115*, 11559–11624. [CrossRef] [PubMed]
26. Bengoechea, M.O.; Agirre, I.; Iriondo, A.; Lopez-Urionabarrenechea, A.; Requies, J.M.; Agirrezabal-Telleria, I.; Bizkarra, K.; Barrio, V.L.; Cambra, J.F. Heterogeneous Catalyzed Thermochemical Conversion of Lignin Model Compounds: An Overview. *Top. Curr. Chem.* **2019**, *377*, 36. [CrossRef] [PubMed]
27. Dutta, S.; Wu, C.W.; Saha, B. Emerging strategies for breaking the 3D amorphous network of lignin. *Catal. Sci. Technol.* **2014**, *4*, 3785–3799. [CrossRef]

28. Xu, C.; Arancon, R.A.D.; Labidi, J.; Luque, R. Lignin depolymerisation strategies: Towards valuable chemicals and fuels. *Chem. Soc. Rev.* **2014**, *43*, 7485–7500. [CrossRef]
29. Ma, R.; Xu, Y.; Zhang, X. Catalytic oxidation of biorefinery lignin to value-added chemicals to support sustainable biofuel production. *ChemSusChem* **2015**, *8*, 24–51. [CrossRef]
30. Cheng, C.; Wang, J.; Shen, D.; Xue, J.; Guan, S.; Gu, S.; Luo, K.H. Catalytic oxidation of lignin in solvent systems for production of renewable chemicals: A review. *Polymers* **2017**, *9*, 240. [CrossRef] [PubMed]
31. Sun, Z.; Fridrich, B.; de Santi, A.; Elangovan, S.; Barta, K. Bright side of lignin depolymerization: Toward new platform chemicals. *Chem. Rev.* **2018**, *118*, 614–678. [CrossRef] [PubMed]
32. QMargellou, A.; Triantafyllidis, K.S. Catalytic Transfer Hydrogenolysis Reactions for Lignin Valorization to Fuels and Chemicals. *Catalysts* **2019**, *9*, 43. [CrossRef]
33. Jing, Y.; Dong, L.; Guo, Y.; Liu, X.; Wang, Y. Chemicals from lignin: A review of the catalytic conversion involving hydrogen. *ChemSusChem* **2020**, *13*, 4181–4198. [CrossRef]
34. Sudarsanam, P.; Duolikun, T.; Babu, P.S.; Rokhum, L.; Johan, M.R. Recent developments in selective catalytic conversion of lignin into aromatics and their derivatives. *Biomass Convers. Bior.* **2020**, *10*, 873–883. [CrossRef]
35. Shivhare, A.; Jampaiah, D.; Bhargava, S.K.; Lee, A.F.; Srivastava, R.; Wilson, K. Hydrogenolysis of Lignin-Derived Aromatic Ethers over Heterogeneous Catalysts. *ACS Sustain. Chem. Eng.* **2021**, *9*, 3379–3407. [CrossRef]
36. Wang, D.; Wang, Y.; Li, X.; Chen, L.; Li, G.; Li, X. Lignin Valorization: A Novel in Situ Catalytic Hydrogenolysis Method in Alkaline Aqueous Solution. *Energy Fuels* **2018**, *32*, 7643–7651. [CrossRef]
37. Shu, R.; Xu, Y.; Chen, P.; Ma, L.; Zhang, Q.; Zhou, L.; Wang, C. Mild Hydrogenation of Lignin Depolymerization Products Over Ni/SiO2 Catalyst. *Energy Fuels* **2017**, *31*, 7208–7213. [CrossRef]
38. Kristianto, I.; Limarta, S.O.; Lee, H.; Ha, J.M.; Suh, D.J.; Jae, J. Effective depolymerization of concentrated acid hydrolysis lignin using a carbon-supported ruthenium catalyst in ethanol/formic acid media. *Bioresour. Technol.* **2017**, *234*, 424–431. [CrossRef]
39. Wang, J.; Li, W.; Wang, H.; Ma, Q.; Li, S.; Chang, H.; Jameel, H. Liquefaction of kraft lignin by hydrocracking with simultaneous use of a novel dual acid-base catalyst and a hydrogenation catalyst. *Bioresour. Technol.* **2017**, *243*, 100–106. [CrossRef]
40. Shu, R.; Long, J.; Xu, Y.; Ma, L.; Zhang, Q.; Wang, T.; Wang, C.; Yuan, Z.; Wu, Q. Investigation on the structural effect of lignin during the hydrogenolysis process. *Bioresour. Technol.* **2016**, *200*, 14–22. [CrossRef]
41. Joffres, B.; Nguyen, M.T.; Laurenti, D.; Souchon, V.; Charon, N.; Daudin, A.; Quignard, A.; Geantet, C. Lignin hydroconversion on MoS2-based supported catalyst: Comprehensive analysis of products and reaction scheme. *Appl. Catal. B Environ.* **2016**, *184*, 153–162. [CrossRef]
42. McVeigh, A.; Bouxin, F.P.; Jarvis, M.C.; Jackson, S.D. Catalytic depolymerisation of isolated lignin to fine chemicals: Part 2—process optimisation. *Catal. Sci. Technol.* **2016**, *6*, 4142–4150. [CrossRef]
43. Struven, J.O.; Meier, D. Hydrocracking of organosolv lignin in subcritical water to useful phenols employing various Raney nickel catalysts. *ACS Sustain. Chem. Eng.* **2016**, *4*, 3712–3721. [CrossRef]
44. Meier, D.; Berns, J.; Faix, O.; Balfanz, U.; Baldauf, W. Hydrocracking of organocell lignin for phenol production. *Biomass Bioenergy* **1994**, *7*, 99–105. [CrossRef]
45. Zhang, J.; Teo, J.; Chen, X.; Asakura, H.; Tanaka, T.; Teramura, K.; Yan, N. A series of NiM (M = Ru, Rh, and Pd) bimetallic catalysts for effective lignin hydrogenolysis in water. *ACS Catal.* **2014**, *4*, 1574–1583. [CrossRef]
46. Barta, K.; Warner, G.R.; Beach, E.S.; Anastas, P.T. Depolymerization of organosolv lignin to aromatic compounds over Cu-doped porous metal oxides. *Green. Chem.* **2014**, *16*, 191–196. [CrossRef]
47. Kloekhorst, A.; Heeres, H.J. Catalytic hydrotreatment of alcell lignin using supported Ru, Pd, and Cu catalysts. *ACS Sustain. Chem. Eng.* **2015**, *3*, 1905–1914. [CrossRef]
48. Kasakov, S.; Shi, H.; Camaioni, D.M.; Zhao, C.; Baráth, E.; Jentys, A.; Lercher, J.A. Reductive deconstruction of organosolv lignin catalyzed by zeolite supported nickel nanoparticles. *Green Chem.* **2015**, *17*, 5079–5090. [CrossRef]
49. Gao, F.; Webb, J.D.; Sorek, H.; Wemmer, D.E.; Hartwig, J.F. Fragmentation of Lignin Samples with Commercial Pd/C under Ambient Pressure of Hydrogen. *ACS Catal.* **2016**, *6*, 7385–7392. [CrossRef]
50. Hakonen, K.J.; González Escobedo, J.L.; Meriö-Talvio, H.; Hashmi, S.F.; Karinen, R.S.; Lehtonen, J. Ethanol organosolv lignin depolymerization with hydrogen over a Pd/C catalyst. *ChemistrySelect* **2018**, *3*, 1761–1771. [CrossRef]
51. Tymchyshyn, M.; Yuan, Z.; Zhang, Y.; Xu, C.C. Catalytic hydrodeoxygenation of guaiacol for organosolv lignin depolymerization—Catalyst screening and experimental validation. *Fuel* **2019**, *254*, 115664. [CrossRef]
52. Figueirêdo, M.B.; Venderbosch, R.H.; Deuss, P.J.; Heeres, H.J. A Two-Step Approach for the Conversion of Technical Lignins to Biofuels. *Adv. Sustain. Syst.* **2020**, *4*, 1900147. [CrossRef]
53. Wang, D.; Wang, W.; Lv, W.; Xu, Y.; Liu, J.; Wang, H.; Wang, C.; Ma, L. The protection of C−O bond of pine lignin in different organic solvent systems. *Chemistry* **2020**, *5*, 3850–3858. [CrossRef]
54. Skaates, J.M.; Kay, W.B. The phase relations of binary systems that form azeotropes N-alkyl alcohol-benzene systems: Methanol through n-butanol. *Chem. Eng. Sci.* **1964**, *19*, 431–444. [CrossRef]
55. Levenspiel, O. Reazioni catalizzate da solidi. In *Ingegneria Delle Reazioni Chimiche*, 2nd ed.; Ambrosiana: Milan, Italy, 1978; p. 471, Chapter 14.

56. Bjelić, A.; Grilc, M.; Likozar, B. Hydrogenation and hydrodeoxygenation of aromatic lignin monomers overMe/C catalysts: Mechanisms, reaction micro-kinetic modelling and quantitative structure-activity relationships. *Chem. Eng.* **2019**, *359*, 305–320. [CrossRef]
57. Bowker, M.; Petts, R.W.; Waugh, K.C. Temperature-programmed desorption studies of alcohol decomposition on ZnO: 1-propanol, 1-butanol and 2-butanol. *J. Catal.* **1986**, *99*, 53–61. [CrossRef]
58. Cai, J.; Zhang, L.; Zhang, F.; Wang, Z.; Cheng, Z.; Yuan, W.; Qi, F. Experimental and kinetic modeling study of n-butanol pyrolysis and combustion. *Energy Fuels* **2012**, *26*, 5550–5568. [CrossRef]
59. Bimbela, F.; Oliva, M.; Ruiz, J.; García, L.; Arauzo, J. Catalytic steam reforming of model compounds of biomass pyrolysis liquids in fixed bed: Acetol and n-butanol. *J. Anal. Appl. Pyrolysis* **2009**, *85*, 204–213. [CrossRef]